Bifurcations and Exact Solutions of the Raman Soliton Model in Nanoscale Optical Waveguides with Metamaterials*

Yan Zhou[1,†] and Jinsen Zhuang[1]

Abstract In this paper, we study Raman soliton model in nanoscale optical waveguides with metamaterials, having polynomial law non-linearity. By using the bifurcation theory method of dynamic systems to the equations of $\phi(\xi)$, under 24 different parameter conditions, we obtain bifurcations of phase portraits and different traveling wave solutions including periodic solutions, homoclinic and heteroclinic solutions for planar dynamic systems of the Raman soliton model. Under different parameter conditions, 24 exact explicit parametric representations of the traveling wave solutions are derived. The dynamic behaviors of these traveling wave solutions are meaningful and helpful for us to understand the physical structures of the model.

Keywords Raman soliton model, Planar dynamic systems, Bifurcations of phase portraits, Traveling wave solutions.

MSC(2010) 34C60, 35Q51, 35C05, 35C07, 35C08.

1. Introduction

With the development of communication technology, optical communication is considered to be the most promising communication method that transmits signals by using optical waves in optical waveguides. As early as 1973, A. Hasegawa and F. Tappert proposed the concept of "optical soliton", which is an optical pulse wave maintaining its amplitude, shape and speed after colliding with other similar solitons [5]. Meanwhile, it was proved theoretically that the optical soliton can be propagated, when the dispersion effect and the nonlinear self-phase modulation effect reach a balance in the fiber. Therefore, the propagation of stable optical solitons has become the focus of current research in nonlinear optics [5].

In practical applications, we need to consider the loss of optical pulse wave energy during signal transmission. Many optical metamaterials (MMS) with abundant optical properties are used as optical fibers, which have linear or nonlinear electromagnetic properties [14, 15]. Some MMS with the negative dielectric constant and magnetic permeability properties are called double negative material (DNG).

———————————————
[†]the corresponding author.
  Email address: zy4233@hqu.edu.cn(Y. Zhou), zzjinsen@hqu.edu.cn(J. Zhuang)
[1]School of Mathematical Sciences, Huaqiao University, Quanzhou, Fujian 362021, China

Raman scattering can occur when the optical pulse signal transmits in these negative exponential DNG materials, which results in some modulation instability and affects the propagation of soliton. Raman soliton is the optical soliton pulse wave obtained by modulating Raman scattering effect and nonlinear effect in the transmission [13, 18].

Xiang [18] derived the propagation equation of Raman solitons in MMS by Maxwell equation, which is the dimensionless and nonlinear Schrodinger equation:

$$iq_t + aq_{xx} + (c_1|q|^2 + c_2|q|^4 + c_3|q|^6)q$$
$$= i\alpha q_x + i\lambda(|q|^2 q)_x + i\nu(|q|^2)_x q + \theta_1(|q|^2 q)_{xx} + \theta_2|q|^2 q_{xx} + \theta_3 q^2 q_{xx}^*, \qquad (1.1)$$

where $a \neq 0$, $q(x,t)$ is the complex-valued wave function with the independent variables x and t(where x is the spatial variable, and t is the temporal variable). The first term represents the temporal evolution of nonlinear wave, while the coefficient a is the group velocity dispersion (GVD). The coefficients c_j for $j = 1, 2, 3$ correspond to the nonlinear terms. Meanwhile, they form polynomial law nonlinearity. It must be noted here that when $c_2 = c_3 = 0$ and $c_1 \neq 0$, the equation (1.1) collapses to the Kerr-law nonlinearity. However, if $c_3 = 0$, $c_1 \neq 0$ and $c_2 \neq 0$, one arrives at parabolic-law nonlinearity. Thus, polynomial law stands as an extension to Kerr-law and parabolic-law. On the right-hand side of (1.1), α represents the coefficient of inter-modal dispersion. This arises when the group velocity of light propagating through a metamaterial is dependent on the propagation mode in addition to chromatic dispersion. The factors λ and ν are accounted for self-steepening for preventing shock-waves and nonlinear dispersion. Finally, the terms with θ_j for $j = 1, 2, 3$ arise in the context of optical metamaterials.

A large class of solitons and ultrashort pulse propagation can be obtained by modulating the linear and nonlinear term coefficients in the propagation equation (1.1) [13, 18]. In 2014, By using the function variable method and first integral method, A. Biswas et al. [3] gave a small number of periodic wave solutions and soliton solutions including light and dark solitons when equation (1.1) has Kerr-law nonlinearity. Subsequently, in the paper [1] published in the same year, A. Biswas et al. used the experimental method to demonstrate the propagation of solitons in MMS, and found that the soliton energy dissipation was caused by the high loss of this double negative material. In addition, by the aid of ansatz method, they obtained some light and dark solitons of equation (1.1). Furthermore, by employing the simple equation method, they found some exact wave solutions of the equation (1.1) including some solitons and period solutions for the Kerr-law nonlinearity [2]. After years, E. V. Krishnan et al. used the mapping function method to drive some periodic wave solutions and solitary wave solutions of the equation (1.1) with Kerr-law nonlinearity and parabolic-law nonlinearity [6] respectively. These solutions obtained in [6] are richer than the solutions obtained by A. Biswas et al. in 2014. Later, M. Veljkovic et al. [17] gave the parameter conditions of ultrashort pulses and numerical simulations of solitons by using set variables. In 2015, Y. Xu and A. Biswas et al. [20] applied the traveling wave hypothesis to model (1.1) for the first time. They set that equation (1.1) has traveling wave solutions with Kerr-law and parabolic-law. Then, in 2016, by using the same method, Y. Xu et al. [19] gave the exact implicit solutions of equation (1.1) with the third kind of elliptic integral form, and made some numerical simulations. In [16], by employing the improved modified extended tanh-function method, the extended trial equation method, the extended Jacobi elliptic function expansion method and the exp (η)-

expansion method respectively, they discussed traveling wave solutions of equation (1.1) with the parabolic law nonlinear and obtain some exact solutions. However, these studies have not found all possible bifurcations of system, exact explicit parametric representations and dynamic behaviors of all traveling wave solutions for equation (1.1).

In this paper, the dynamic systems method developed in [7–12] is employed to study the propagation equation (1.1). First, we transform the nonlinear Schrodinger PDE equation into an ODE system through traveling wave hypothesis, and obtain equivalent planar dynamic systems. Secondly, we use the bifurcation theory of nonlinear dynamic systems to study bifurcations of the planar dynamic systems, and obtain physical phase portraits of the system. Lastly, we give all possible exact solutions according to the phase protraits and give the exact parametric representations of solutions. Compared with previous results in [1–3, 6, 17, 19, 20], by using the dynamic systems method, we obtain not only the all possible bifurcations of the equation (1.1), but also traveling wave solutions as much as possible under various parameters conditons.

Recently, in paper [22], we considered the case of $c_1 \neq 0, c_2 = c_3 = 0$ when $\theta_1 \neq 0, 3\theta_1 + \theta_2 + \theta_3 \neq 0$ in equation (1.1) and obtained possible bifurcations and exact solutions for the equation (1.1) with Kerr-law nonlinearity by using the bifurcation theory of dynamic systems. When $\theta_1 \neq 0, 3\theta_1 + \theta_2 + \theta_3 \neq 0$, we discussed further the case $c_1 \neq 0, c_2 \neq 0, c_3 = 0$ in [21] for equation (1.1) which has the parabolic-law nonlinearity and obtained possible bifurcations, exact explicit parametric representations and dynamic behaviors of solutions for equation (1.1). Here, we discuss the case $\theta_1 = 0, \theta_2 + \theta_3 = 0$ in equation (1.1) with polynomial-law nonlinearity. We derive the corresponding planar dynamic systems of equation (1.1) in Section 2, discuss the bifurcations of phase portraits of equation (1.1) in Section 3 and give the different exact solutions of equation (1.1) in Section 4 under different parameter conditions.

2. Planar dynamic systems

Consider the solutions of equation (1.1) having the form

$$q(x,t) = \phi(\eta)\exp(i(-kx + \omega t)), \quad \eta = x - vt. \tag{2.1}$$

When $\theta_1 = 0, \theta_2 + \theta_3 = 0$, substituting (2.1) into (1.1) and separating the real and imaginary parts, we have

$$a\phi'' - a_1\phi + a_3\phi^3 + c_2\phi^5 + c_3\phi^7 = 0, \tag{2.2}$$

$$(v + \alpha + 2ak) + [3\lambda + 2\nu - 4\theta_2 k]\phi^2 = 0, \tag{2.3}$$

where $a_1 = \omega + \alpha k + ak^2, a_3 = c_1 - k\lambda$, the notation $\phi' = \frac{d\phi}{d\eta}$. From the imaginary part equation (2.3), upon setting the coefficients of linearly independent functions to zero, it gives the relations:

$$v = -(\alpha + 2ak), \quad 3\lambda + 2\nu = 2k(\theta_2 - \theta_3). \tag{2.4}$$

Making the parameter transformation: $\alpha_0 = \frac{a_1}{a}, \alpha_2 = \frac{-a_3}{a}, \alpha_4 = \frac{-c_2}{a}, \alpha_6 = \frac{-c_3}{a}$, then the equation (2.2) is equivalent to the following planar dynamic system:

$$\frac{d\phi}{d\eta} = z, \quad \frac{dz}{d\eta} = \phi(\alpha_0 + \alpha_2\phi^2 + \alpha_4\phi^4 + \alpha_6\phi^6). \tag{2.5}$$

System (2.5) is a four-parameter integrable planar dynamic system depending on the parameter group $(\alpha_0, \alpha_2, \alpha_4, \alpha_6)$. We make the transformation: $\eta = \frac{\xi}{\sqrt{|\alpha_6|}}, z = \sqrt{|\alpha_6|}y$, then, system (2.5) becomes system (2.6) for $\alpha_6 > 0$ and system (2.7) for $\alpha_6 < 0$ as follows:

$$\frac{d\phi}{d\xi} = y, \quad \frac{dy}{d\xi} = \phi(b_0 + b_2\phi^2 + b_4\phi^4 + \phi^6). \tag{2.6}$$

$$\frac{d\phi}{d\xi} = y, \quad \frac{dy}{d\xi} = -\phi(b_0 + b_2\phi^2 + b_4\phi^4 + \phi^6). \tag{2.7}$$

where $b_0 = \frac{\alpha_0}{\alpha_6}, b_2 = \frac{\alpha_2}{\alpha_6}, b_4 = \frac{\alpha_4}{\alpha_6}$. We can see that systems (2.6) and (2.7) are two three-parameter integrable planar dynamic systems depending on the same parameter group (b_0, b_2, b_4).

Systems (2.6) and (2.7) have the following first integrals:

$$H_1(\phi, y) = y^2 - b_0\phi^2 - \frac{b_2}{2}\phi^4 - \frac{b_4}{3}\phi^6 - \frac{1}{4}\phi_j^8 = h, \tag{2.8}$$

$$H_2(\phi, y) = y^2 + b_0\phi^2 + \frac{b_2}{2}\phi^4 + \frac{b_4}{3}\phi^6 + \frac{1}{4}\phi_j^8 = h. \tag{2.9}$$

We use the method of dynamic systems to investigate the dynamic behaviors of systems (2.6) and (2.7), and find all possible bifurcations and exact explicit parametric representations for the traveling wave solutions of systems (2.6) and (2.7). We will see that the solutions have very abounded dynamic behaviors.

3. Bifurcations of phase portraits of systems (2.6) and (2.7)

In this section, we consider the bifurcations of phase portraits of systems (2.6) and (2.7) depending on the parameter group (b_0, b_2, b_4).

Clearly, systems (2.6) and (2.7) have the same equilibrium points. They always have the equilibrium point $E_0(0,0)$. Write $f_6(\phi) = b_0 + b_2\phi^2 + b_4\phi^4 + \phi^6$. The other equilibrium points $(\phi_j, 0)$ of them depend on the number of zeros ϕ_j of the six-degree algebraic equation $f_6(\phi) = 0$. Make $g_3(p) = b_0 + b_2p + b_4p^2 + p^3$. We notice that if p_j is positive zero of the cubic algebraic equation $g_3(p) = 0$, then $\pm\sqrt{p_j}$ are two symmetrical zeros of the six-degree algebraic equation $f_6(\phi) = 0$. Let $q = \frac{1}{3}b_2 - \frac{1}{9}b_4^2$, $r = \frac{1}{6}(b_2b_4 - 3b_0) - \frac{1}{27}b_4^3$. Then, when

$$S = q^3 + r^2 = \frac{1}{27}b_2^3 - \frac{1}{108}b_2^2b_4^2 - \frac{1}{6}b_0b_2b_4 + \frac{1}{4}b_0^2 + \frac{1}{27}b_0b_4^3 < 0,$$

$g_3(p) = 0$ has three simple real zeros. When $S = 0$, $g_3(p) = 0$ has a simple real zero and a double real zero. When $S > 0$, $g_3(p) = 0$ has only one real zero.

For a given fixed $b_0 \neq 0$, in the (b_2, b_4) parametric plane, the function $S(b_2, b_4) = 0$ defines a curve shown in Figures 1(a) and 1(b), which has three branches and partitions the $(b_2, b_4)-$parameter plane into three regions. It is easy to prove that the curve defined by $S(b_2, b_4) = 0$ has a cusp point at $(3b_0^{\frac{2}{3}}, 3b_0^{\frac{1}{3}})$. In regions (I_2) and (I_3), when $b_0 > 0$, regions $(\hat{I}_2)$ and $(\hat{I}_3)$ when $b_0 < 0$, we have $S(b_2, b_4) < 0$. In region (I_1) for $b_0 > 0$, region $(\hat{I}_1)$ for $b_0 < 0$, $S(b_2, b_4) > 0$.
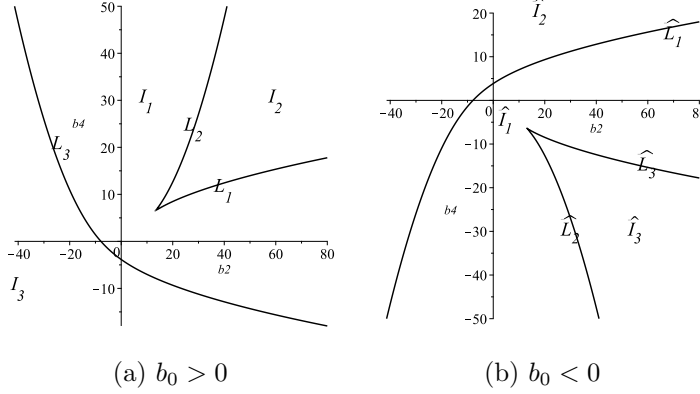

(a) $b_0 > 0$ (b) $b_0 < 0$

Figure 1 The partition of the $(b_2, b_4)-$parametric plane

Let $M_i(\phi_j, 0), (i = 1, 2)$ be the coefficient matrices of the linearized systems of systems (2.6) and (2.7) at positive equilibrium point $E_j(\phi_j, 0)$, we have

$$J_1(0,0) = det M_1(0,0) = -b_0, J_2(0,0) = det M_2(0,0) = b_0,$$

$$J_1(\phi_j, 0) = det M_1(\phi_j, 0) = -(b_0 + 3b_2\phi_j^2 + 5b_4\phi_j^4 + 7\phi_j^6),$$

$$J_2(\phi_j, 0) = det M_2(\phi_j, 0) = b_0 + 3b_2\phi_j^2 + 5b_4\phi_j^4 + 7\phi_j^6.$$

Where $J_1(0,0) = -b_0$ and $J_2(0,0) = b_0$ imply that for $b_0 < 0$, equilibrium point $E_0(0,0)$ is a center point of system (2.6) and a saddle point of system (2.7). While when $b_0 > 0$, equilibrium point $E_0(0,0)$ is a saddle point of system (2.6) and a center point of system (2.7). Equilibrium points $E_{\pm j}(\phi_{\pm j}, 0)$ are either two symmetrical center points or two symmetrical saddle points.

We write that $h_{10} = H_1(0,0) = 0, h_{20} = H_2(0,0) = 0, h_{1j} = H_1(\phi_j, 0) = -b_0\phi_j^2 - \frac{b_2}{2}\phi_j^4 - \frac{b_4}{3}\phi_j^6 - \frac{1}{4}\phi_j^8, h_{2j} = H_2(\phi_j, 0) = b_0\phi_j^2 + \frac{b_2}{2}\phi_j^4 + \frac{b_4}{3}\phi_j^6 + \frac{1}{4}\phi_j^8$.

By the above information, we obtain the following lemma and bifurcations of the phase portraits of systems (2.6) and (2.7) shown in Figure 2–Figure 5.

Lemma 3.1. *When $b_0 > 0$, the origin $E_0(0,0)$ is a saddle point of system (2.6). When $(b_2, b_4) \in I_1$ or $(b_2, b_4) \in L_1$ or $(b_2, b_4) \in L_2$ or $(b_2, b_4) \in I_2$ or $(b_2, b_4) = (3b_0^{2/3}, 3b_0^{1/3})$, we have phase portrait Figure 2(a). When $(b_2, b_4) \in L_3$, we have phase portrait Figure 2(b). When $(b_2, b_4) \in I_3, h_{11} > 0$, we have phase portrait Figure 2(c). When $(b_2, b_4) \in I_3, h_{11} = 0$, we have phase portrait Figure 2(d). When $(b_2, b_4) \in I_3, h_{11} < 0$, we have phase portrait Figure 2(e).*
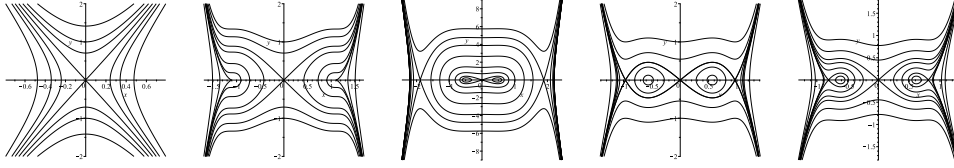
Figure 2 The bifurcations of phase portraits of system (2.6) for $b_0 > 0$

(a) $(b_2, b_4) \in I_1$ or $(b_2, b_4) \in L_1$ or $(b_2, b_4) \in L_2$ or $(b_2, b_4) \in I_2$ or $(b_2, b_4) = (3b_0^{2/3}, 3b_0^{1/3})$. (b) $(b_2, b_4) \in L_3$. (c) $(b_2, b_4) \in I_3, h_{11} > 0$. (d) $(b_2, b_4) \in I_3, h_{11} = 0$. (e) $(b_2, b_4) \in I_3, h_{11} < 0$.

Lemma 3.2. *When $b_0 < 0$, the origin $E_0(0, 0)$ is a center point of system (2.6). When $(b_2, b_4) \in \hat{I}_1$ or $(b_2, b_4) \in \hat{L}_1$ or $(b_2, b_4) \in \hat{I}_2$, we have phase portrait Figure 3(a). When $(b_2, b_4) = (3b_0^{2/3}, 3b_0^{1/3})$, we have phase portrait Figure 3(b). When $(b_2, b_4) \in \hat{L}_2$, we have phase portrait Figure 3(c). When $(b_2, b_4) \in \hat{I}_3, h_{11} > h_{13}$, we have phase portrait Figure 3(d). When $(b_2, b_4) \in \hat{I}_3, h_{11} = h_{13}$, we have phase portrait Figure 3(e). When $(b_2, b_4) \in \hat{I}_3, h_{11} < h_{13}$, we have phase portrait Figure 3(f). When $(b_2, b_4) \in \hat{L}_3$, we have phase portrait Figure 3(g).*
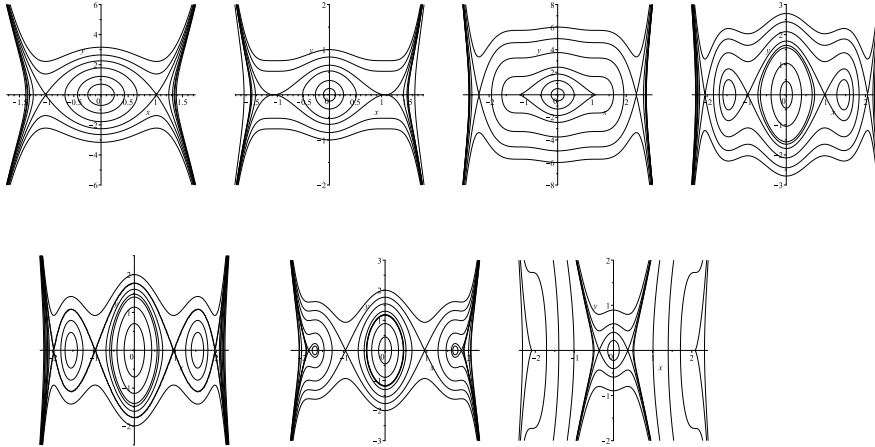

Figure 3 The bifurcations of phase portraits of system (2.6) for $b_0 < 0$

(a) $(b_2, b_4) \in \hat{I}_1$ or $(b_2, b_4) \in \hat{L}_1$ or $(b_2, b_4) \in \hat{I}_2$. (b) $(b_2, b_4) = (3b_0^{2/3}, 3b_0^{1/3})$. (c) $(b_2, b_4) \in \hat{L}_2$. (d) $(b_2, b_4) \in \hat{I}_3, h_{11} > h_{13}$. (e) $(b_2, b_4) \in \hat{I}_3, h_{11} = h_{13}$. (f) $(b_2, b_4) \in \hat{I}_3, h_{11} < h_{13}$. (g) $(b_2, b_4) \in \hat{L}_3$.

Lemma 3.3. *When $b_0 > 0$, the origin $E_0(0, 0)$ is a center point of system (2.7). When $(b_2, b_4) \in I_1$ or $(b_2, b_4) \in L_1$ or $(b_2, b_4) \in L_2$ or $(b_2, b_4) \in I_2$ or $(b_2, b_4) = (3b_0^{2/3}, 3b_0^{1/3})$, we have phase portrait Figure 4(a). When $(b_2, b_4) \in L_3$, we have phase portrait Figure 4(b). When $(b_2, b_4) \in I_3, h_{21} < 0$, we have phase portrait Figure 4(c). When $(b_2, b_4) \in I_3, h_{21} = 0$, we have phase portrait Figure 4(d). When $(b_2, b_4) \in I_3, h_{21} > 0$, we have phase portrait Figure 4(e).*
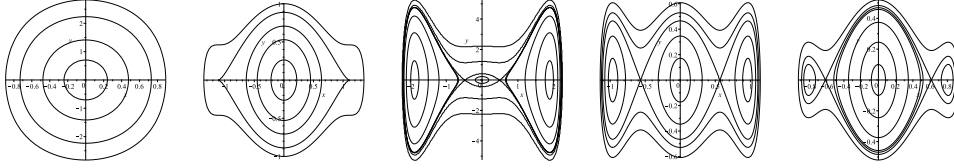
Figure 4 The bifurcations of phase portraits of system (2.7) for $b_0 > 0$

(a) $(b_2, b_4) \in I_1$ or $(b_2, b_4) \in L_1$ or $(b_2, b_4) \in L_2$ or $(b_2, b_4) \in I_2$ or $(b_2, b_4) = (3b_0^{2/3}, 3b_0^{1/3})$. (b) $(b_2, b_4) \in L_3$. (c) $(b_2, b_4) \in I_3, h_{21} < 0$. (d) $(b_2, b_4) \in I_3, h_{21} = 0$. (e) $(b_2, b_4) \in I_3, h_{21} > 0$.

Lemma 3.4. *When $b_0 < 0$, the origin $E_0(0, 0)$ is a saddle point of system (2.7). When $(b_2, b_4) \in \hat{I}_1$ or $(b_2, b_4) \in \hat{L}_1$ or $(b_2, b_4) \in \hat{I}_2$, we have phase portrait Figure 5(a). When $(b_2, b_4) = (3b_0^{2/3}, 3b_0^{1/3})$, we have phase portrait Figure 5(b). When $(b_2, b_4) \in \hat{L}_2$, we have phase portrait Figure 5(c). When $(b_2, b_4) \in \hat{I}_3, h_{21} < h_{23}$, we have phase portrait Figure 5(d). $(b_2, b_4) \in \hat{I}_3, h_{21} = h_{23}$, we have phase portrait Figure 5(e). When $(b_2, b_4) \in \hat{I}_3, h_{21} > h_{23}$, we have phase portrait Figure 5(f). When $(b_2, b_4) \in \hat{L}_3$, we have phase portrait Figure 5(g).*
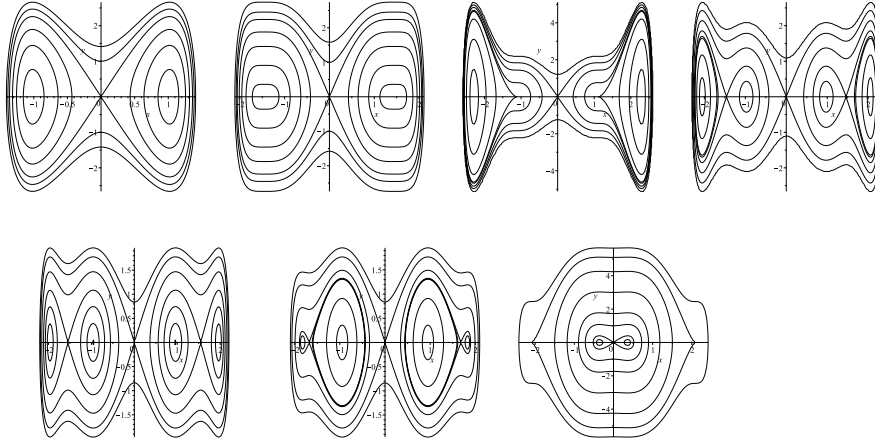

Figure 5 The bifurcations of phase portraits of system (2.7) for $b_0 < 0$

(a) $(b_2, b_4) \in \hat{I}_1$ or $(b_2, b_4) \in \hat{L}_1$ or $(b_2, b_4) \in \hat{I}_2$. (b) $(b_2, b_4) = (3b_0^{2/3}, 3b_0^{1/3})$. (c) $(b_2, b_4) \in \hat{L}_2$. (d) $(b_2, b_4) \in \hat{I}_3, h_{21} < h_{23}$. (e) $(b_2, b_4) \in \hat{I}_3, h_{21} = h_{23}$. (f) $(b_2, b_4) \in \hat{I}_3, h_{21} > h_{23}$. (g) $(b_2, b_4) \in \hat{L}_3$.

4. Exact parametric representations of solutions of systems (2.6) and (2.7)

In this section, we analyze the level curves defined by $H_i(\phi, y) = h, (i = 1, 2)$ in (2.8) and (2.9), and obtain all possible exact solutions of equation (1.1) for different cases in Section 2.

Notice that $H_i(\phi, y) = h, (i = 1, 2)$ give rise to

$$y^2 = \pm(b_0\phi^2 + \frac{b_2}{2}\phi^4 + \frac{b_4}{3}\phi^6 + \frac{1}{4}\phi^8) + h \equiv F_8(\phi). \qquad (4.1)$$

Obviously, if and only if polynomial $F_8(\phi)$ can be decomposed into a product of quadratic factors, the integral $\int_{\phi_0}^{\phi} \frac{1}{\sqrt{F_8(\phi)}}$ can be solved (see [4]).

4.1. Exact parametric representations of solutions of system (2.6).

Theorem 4.1. *System (2.6) has the following traveling wave solutions for $b_0 > 0$:*
  (i) When $b_0 > 0$, $(b_2, b_4) \in I_3, h_{11} > 0$, system (2.6) has homoclinic solutions

$$\phi(\chi) = \pm\frac{\phi_M\sqrt{1-\alpha_1^2 sn^2(\chi,k)}}{dn(\chi,k)}, \quad \chi \in \left(-sn^{-1}\sqrt{\frac{\phi_M^2(r_1^2+r_2^2)}{r_1^2(\phi_M^2+r_2^2)}}, sn^{-1}\sqrt{\frac{\phi_M^2(r_1^2+r_2^2)}{r_1^2(\phi_M^2+r_2^2)}}\right),$$
$$\xi(\chi) = \frac{2}{r_1^2\sqrt{(r_1^2+r_2^2)}}\left[\chi + \frac{r_1^2-\phi_M^2}{\phi_M^2}\Pi(\arcsin(sn(\chi,k),\alpha_1^2,k))\right], \qquad (4.2)$$

where $\alpha_1^2 = \frac{r_1^2(\phi_M^2+r_2^2)}{\phi_M^2(r_1^2+r_2^2)}, k^2 = \frac{\phi_M^2+r_2^2}{r_1^2+r_2^2}$.
  In this case, system (2.6) also has heteroclinic solutions

$$\phi(\chi) = \pm\frac{\rho\bar{\rho}(1-cn(\chi,k))}{sn(\chi,k)}, \quad \chi \in \left(-cn^{-1}(\frac{A_1-\phi_1^2}{A_1+\phi_1^2}), cn^{-1}(\frac{A_1-\phi_1^2}{A_1+\phi_1^2})\right),$$
$$\xi(\chi) = \frac{1}{(\phi_1^2+A_1)\sqrt{A_1}}\left\{\chi + \frac{2A_1}{(1-\alpha_2^2)(\phi_1^2-A_1)}[\Pi(\arccos(cn(\chi,k),\frac{\alpha_2^2}{\alpha_2^2-1},k)) - \alpha_2 f_1]\right\}, \qquad (4.3)$$

where $a_1^2 = -\frac{(\rho^2-\bar{\rho}^2)}{4}, b_1 = \frac{\rho^2+\bar{\rho}^2}{2}, A_1^2 = b_1^2 + a_1^2 = \rho^2\bar{\rho}^2, \alpha_2 = \frac{\phi_1^2+A_1}{\phi_1^2-A_1}, k^2 = \frac{A_1+b_1}{2A_1}$.
  (ii) When $b_0 > 0$, $(b_2, b_4) \in I_3, h_{11} = 0$, system (2.6) has heteroclinic solutions

$$\phi(\chi) = \pm r_1 csch\chi, \quad \chi \in \left(csch^{-1}(\frac{\phi_1}{r_1}), +\infty\right),$$
$$\xi(\chi) = \frac{2}{\phi_1^2}\left[\frac{1}{\sqrt{\phi_1^2+r_1^2}}tanh^{-1}(\sqrt{\frac{r_1^2+\phi^2}{\phi_1^2+r_1^2}}) - \frac{1}{\sqrt{\phi_1^2+r_1^2}}tanh^{-1}(\sqrt{\frac{r_1^2+\phi_2^2}{\phi_1^2+r_1^2}})\right.$$
$$\left. - \frac{1}{r_1}tanh^{-1}(\frac{r_1}{\sqrt{\phi^2+r_1^2}}) + \frac{1}{r_1}tanh^{-1}(\frac{r_1}{\sqrt{\phi_2^2+r_1^2}})\right]. \qquad (4.4)$$

 *(iii) When $b_0 > 0$, $(b_2, b_4) \in I_3, h_{11} < 0$, system (2.6) has homoclinic solutions*

$$\phi(\chi) = \pm\frac{\phi_M}{cn(\chi,k)}, \quad \chi \in \left(-cn^{-1}(\frac{\phi_M}{\phi_1}), cn^{-1}(\frac{\phi_M}{\phi_1})\right),$$
$$\xi(\chi) = \frac{2}{\phi_1^2\sqrt{(r_1^2+\phi_1^2)}}\left[\chi + \frac{\phi_M^2}{\phi_1^2-\phi_M^2}\Pi(\arcsin(sn(\chi,k),\alpha_3^2,k))\right], \qquad (4.5)$$

where $\alpha_3^2 = \frac{\phi_1^2}{\phi_1^2-\phi_M^2}, k^2 = \frac{r_1^2}{r_1^2+\phi_M^2}$.

Remark 4.1. The functions $cn(\cdot, k), sn(\cdot, k), dn(\cdot, k)$ are Jacobin elliptic functions, $\Pi(\cdot, \cdot, k)$ is the elliptic integral of the third kind and the function $f_1(\chi)$ can be seen in [4] (361.54).

Proof. (i) When $b_0 > 0$, $(b_2, b_4) \in I_3, h_{11} > 0$, system (2.6) has phase portrait Figure 2(c). The changes of the level curves defined by $H_1(\phi, y) = h$ in Figure 2(c) are shown as follows:
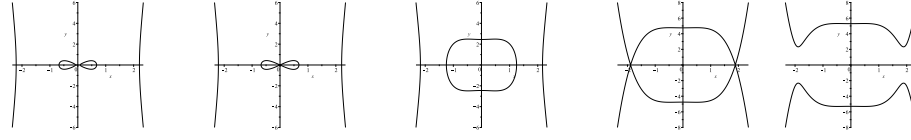
(a) $h_{11} < h < h_{10}$ (b) $h = h_{10}$ (c) $h_{10} < h < h_{12}$ (d) $h = h_{12}$ (e) $h > h_{12}$

Figure 6 The changes of the level curves when $b_0 > 0$, $(b_2, b_4) \in I_3$, $h_{11} > 0$

When $h = 0$, the level curves defined by $H_1(\phi, y) = h$ are two homoclinic orbit loops to the origin and contacting $\phi-$axis in the points $(\pm\phi_M, 0)$ and two open curves which pass through $\phi-$axis at the points $(\pm r_1, 0)$ (Figure 6(b)). Now, for the two homoclinic orbits, we have $y^2 = \frac{1}{4}(r_1^2 - \phi^2)(\phi_M^2 - \phi^2)\phi^2(\phi^2 + r_2^2)$. Substituting it into the first equation of system (2.6) and integrating along the homoclinic orbits, it follows that

$$\xi = \int_u^{\phi_M^2} \frac{du}{u\sqrt{(r_1^2 - u)(\phi_M^2 - u)(u + r_2^2)}}.$$

Therefore, we obtain the parametric representations (4.2) of the homoclinic solutions of system (2.6). The homoclinic solutions have the following wave portrait:
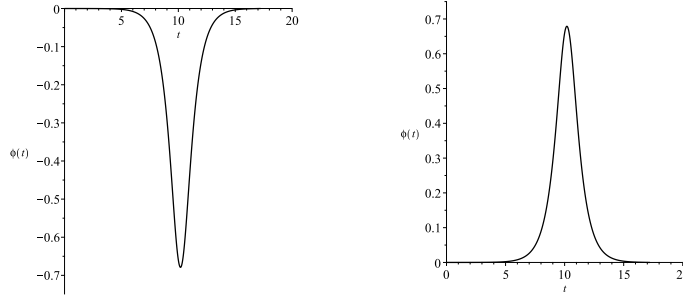
(a) Solitary wave of valley type   (b) Solitary wave of peak type

Figure 7 The solitary wave of system (2.6)

When $h = h_{12}$, the level curves defined by $H_1(\phi, y) = h$ are two heteroclinic orbits connecting to the points $(\pm\phi_1, 0)$ and four stable and unstable manifolds to the points $(\pm\phi_1, 0)$ (Figure 6(d)). Corresponding to the two heteroclinic orbits, we have $y^2 = \frac{1}{4}(\phi_1^2 - \phi^2)(\phi^2 - \rho^2)(\phi^2 - \bar{\rho}^2)$, where ρ and $\bar{\rho}$ are two conjugated complex zeros of (4.1). Substituting it into the first equation of system (2.6) and integrating along the heteroclinic orbits, it follows that

$$\xi = \int_0^u \frac{du}{(\phi_1^2 - u)\sqrt{u(\phi^2 - \rho^2)(\phi^2 - \bar{\rho}^2)}}.$$

Then, we obtain the parametric representations (4.3) of the heteroclinic solutions of system (2.6).

(ii) When $b_0 > 0$, $(b_2, b_4) \in I_3$, $h_{11} = 0$, system (2.6) has phase portrait Figure 2(d). The level curves defined by $H_1(\phi, y) = h_{11}$ are four heteroclinic orbits connecting to the origin and points $(\pm\phi_1, 0)$ and enclosing the equilibrium points

$(\pm\phi_2, 0)$ as well as four stable and unstable manifolds of the points $(\pm\phi_1, 0)$. For the four heteroclinic orbits, we have $y^2 = \frac{1}{4}(\phi_1^2 - \phi^2)^2\phi^2(\phi^2 + r_1^2)$. Substituting it into the first equation of system (2.6) and integrating along the heteroclinic orbits, it follows that

$$\frac{1}{2}\xi = \int_{\phi_2}^{\phi} \frac{d\phi}{(\phi_1^2 - \phi^2)\phi\sqrt{\phi^2 + r_1^2}}.$$

Hence, the four heteroclinic orbits have the parametric representation (4.4) (kink and anti-kink wave solutions).

(iii) When $b_0 > 0, (b_2, b_4) \in I_3, h_{11} < 0$, system (2.6) has phase portrait Figure 2(e). The level curves defined by $H_1(\phi, y) = h_{11}$ are two homoclinic orbits to the points $(\pm\phi_1, 0)$ and passing through $\phi-$axis at the points $(\pm\phi_M, 0)$, and the stable and unstable manifolds of the equilibrium points $(\pm\phi_1, 0)$. Corresponding to the homoclinic orbits, we have $y^2 = \frac{1}{4}(\phi_1^2 - \phi^2)^2(\phi^2 - \phi_M^2)(\phi^2 + r_1^2)$. Substituting it into the first equation of system (2.6) and integrating along the homoclinic orbits, it follows that

$$\xi = \int_{\phi_M^2}^{u} \frac{du}{(\phi_1^2 - u)\sqrt{(u - \phi_M^2)u(u + r_1^2)}}.$$

Therefore, we obtain the parametric representation (4.5) of the solitary wave solutions of system (2.6). □

Theorem 4.2. *System* (2.6) *has the following traveling wave solutions for $b_0 < 0$:*

(i) When $b_0 < 0, (b_2, b_4) = (3b_0^{2/3}, 3b_0^{1/3})$, system (2.6) *has heteroclinic solutions*

$$\begin{aligned} \phi(\chi) &= \pm\phi_1\tanh(\chi), \quad \chi \in [0, +\infty), \\ \xi(\chi) &= \tfrac{1}{4\phi_1^3}\left(\sinh(2\chi) + 2\chi\right). \end{aligned} \tag{4.6}$$

(ii) When $b_0 < 0, (b_2, b_4) \in \hat{L}_2$, system (2.6) *has heteroclinic solutions*

$$\begin{aligned} \phi(\chi) &= \pm\phi_2 sn(\chi, k), \quad \chi \in (-K, K), \\ \xi(\chi) &= \tfrac{2}{r_1\phi_2^2}\Pi(\arcsin(sn(\chi, k), 1, k), \end{aligned} \tag{4.7}$$

where $k^2 = \frac{\phi_2^2}{r_1^2}$.

(iii) When $b_0 < 0, (b_2, b_4) \in \hat{I}_3, h_{11} > h_{13}$, system (2.6) *has periodic wave solution*

$$\begin{aligned} \phi(\chi) &= \pm r_2 sn(\chi, k), \\ \xi(\chi) &= \tfrac{2}{r_1\phi_2^2}\Pi(\arcsin(sn(\chi, k), \hat{\alpha}_1^2, k)), \end{aligned} \tag{4.8}$$

where $\hat{\alpha}_1^2 = \frac{r_2^2}{\phi_2^2}, k^2 = \frac{r_2^2}{r_1^2}$.

In this case, system (2.6) *also has heteroclinic solutions*

$$\begin{aligned} \phi(\chi) &= \pm\phi_M sn(\chi, k), \quad \chi \in \left(-sn^{-1}(\tfrac{\phi_3}{\phi_M}), sn^{-1}(\tfrac{\phi_3}{\phi_M})\right), \\ \xi(\chi) &= \tfrac{2}{r_1\phi_3^2}\Pi(\arcsin(sn(\chi, k), \hat{\alpha}_2^2, k)), \end{aligned} \tag{4.9}$$

where $\hat{\alpha}_2^2 = \frac{\phi_M^2}{\phi_3^2}, k^2 = \frac{\phi_M^2}{r_1^2}$, and homoclinic solutions

$$\phi(\chi) = \pm cd(\chi, k), \quad \chi \in \left(-sn^{-1}\sqrt{\frac{r_1^2(\phi_M^2 - \phi_3^2)}{\phi_M^2(r_1^2 - \phi_3^2)}}, sn^{-1}\sqrt{\frac{r_1^2(\phi_M^2 - \phi_3^2)}{\phi_M^2(r_1^2 - \phi_3^2)}}\right),$$

$$\xi(\chi) = \frac{2}{r_1(r_1^2 - \phi_3^2)}\left[\chi + \frac{\phi_M^2 - r_1^2}{\phi_3^2 - \phi_M^2}\Pi(\arcsin(sn(\chi, k)), \hat{\alpha}_3^2, k)),\right. \tag{4.10}$$

where $\hat{\alpha}_3^2 = \frac{k^2(\phi_3^2 - r_1^2)}{\phi_3^2 - \phi_M^2}, k^2 = \frac{\phi_M^2}{r_1^2}$.

   (iv) When $b_0 < 0, (b_2, b_4) \in \hat{I}_3, h_{11} = h_{13}$, system (2.6) has heteroclinic solutions

$$\phi(\chi) = \pm\frac{(e^\chi - 1)\phi_3}{1 + e^\chi}, \quad \chi \in [0, +\infty),$$

$$\xi(\chi) = \frac{2}{(\phi_1^2 - \phi_3^2)}\left[\frac{\chi}{2\phi_3} - \frac{1}{2\phi_1}\ln\frac{(\phi_1 + \phi_3)e^\chi + \phi_1 - \phi_3}{(\phi_1 - \phi_3)e^\chi + \phi_1 + \phi_3}\right], \tag{4.11}$$

and

$$\phi(\chi) = \pm\frac{(e^\chi - 1)\phi_1}{1 + e^\chi}, \quad \chi \in \left(\ln\frac{\phi_1 + \phi_3}{\phi_1 - \phi_3}, +\infty\right),$$

$$\xi(\chi) = \frac{2}{(\phi_1^2 - \phi_3^2)}\left[\frac{\chi}{2\phi_1} - \frac{1}{2\phi_1}\ln\frac{\phi_2 + \phi_1}{\phi_1 - \phi_2} - \frac{1}{2\phi_3}\ln\frac{\phi_2 - \phi_3}{\phi_2 + \phi_3} + \frac{1}{2\phi_3}\ln\frac{(\phi_1 - \phi_3)e^\chi - \phi_1 - \phi_3}{(\phi_1 + \phi_3)e^\chi - \phi_1 + \phi_3}\right]. \tag{4.12}$$

   (v) When $b_0 < 0, (b_2, b_4) \in \hat{I}_3, h_{11} < h_{13}$, system (2.6) has periodic wave solution

$$\phi(\chi) = \pm r_1 sn(\chi, k),$$

$$\xi(\chi) = \frac{2}{\phi_M\phi_1^2}\Pi(\arcsin(sn(\chi, k)), \hat{\alpha}_4^2, k)), \tag{4.13}$$

where $\hat{\alpha}_4^2 = \frac{r_1^2}{\phi_1^2}, k^2 = \frac{r_1^2}{\phi_M^2}$, and homoclinic solutions

$$\phi(\chi) = \pm\frac{\phi_M dn(\chi, k)}{cn(\chi, k)}, \quad \chi \in \left(-sn^{-1}\sqrt{\frac{\phi_1^2 - \phi_M^2}{\phi_1^2 - r_1^2}}, sn^{-1}\sqrt{\frac{\phi_1^2 - \phi_M^2}{\phi_1^2 - r_1^2}}\right),$$

$$\xi(\chi) = \frac{2}{\phi_M(\phi_1^2 - r_1^2)}\left[\chi + \frac{r_1^2 - \phi_M^2}{\phi_M^2 - \phi_1^2}\Pi(\arcsin(sn(\chi, k)), \hat{\alpha}_5^2, k))\right], \tag{4.14}$$

where $\hat{\alpha}_5^2 = \frac{r_1^2 - \phi_1^2}{\phi_M^2 - \phi_1^2}, k^2 = \frac{r_1^2}{\phi_M^2}$.

Proof.   (i) When $b_0 < 0, (b_2, b_4) = (3b_0^{2/3}, 3b_0^{1/3})$, system (2.6) has phase portrait Figure 3(b). When $h = h_{11}$, the level curves defined by $H_1(\phi, y) = h$ are two heteroclinic orbits connecting to the cusps $(\pm\phi_1, 0)$ and enclosing the origin as well as four stable and unstable manifolds of the equilibrium points $(\pm\phi_1, 0)$. Now, for the heteroclinic orbits, we have $y^2 = \frac{1}{4}(\phi^2 - \phi_1^2)^4$. Substituting it into the first equation of system (2.6) and integrating along the heteroclinic orbits, it follows that

$$\xi = \int_0^\phi \frac{d\phi}{(\phi_1^2 - \phi^2)^2}.$$

Thus, we have the parametric representations (4.6) of heteroclinic solutions.

   (ii) When $b_0 < 0, (b_2, b_4) \in \hat{L}_2$, system (2.6) has phase portrait Figure 3(c). When $h = h_{12} = h_{13}$, the level curves defined by $H_1(\phi, y) = h$ are two heteroclinic orbits connecting to the cusps $(\pm\phi_2, 0)$ and enclosing the origin, and two open curves passing through $\phi-$axis at the points $(\pm r_1, 0)$. Corresponding to the heteroclinic

orbits, we have $y^2 = \frac{1}{4}(\phi_2^2 - \phi^2)^3(r_1^2 - \phi^2)$. Substituting it into the first equation of system (2.6) and integrating along the heteroclinic orbits, it follows that

$$\frac{1}{2}\xi = \int_0^\phi \frac{d\phi}{(\phi_2^2 - \phi^2)\sqrt{(\phi_2^2 - \phi^2)(r_1^2 - \phi^2)}}.$$

Then, we obtain the parametric representations (4.7) of the heteroclinic solutions.

(iii) When $b_0 < 0, (b_2, b_4) \in \hat{I}_3, h_{11} > h_{13}$, system (2.6) has phase portrait Figure 3(d). The changes of the level curves defined by $H_1(\phi, y) = h$ in Figure 3(d) are shown as follows:

(a) $h = h_{12}$ (b) $h_{12} < h < h_{13}$ (c) $h = h_{13}$ (d) $h_{13} < h < h_{11}$

(e) $h = h_{11}$ (f) $h > h_{11}$
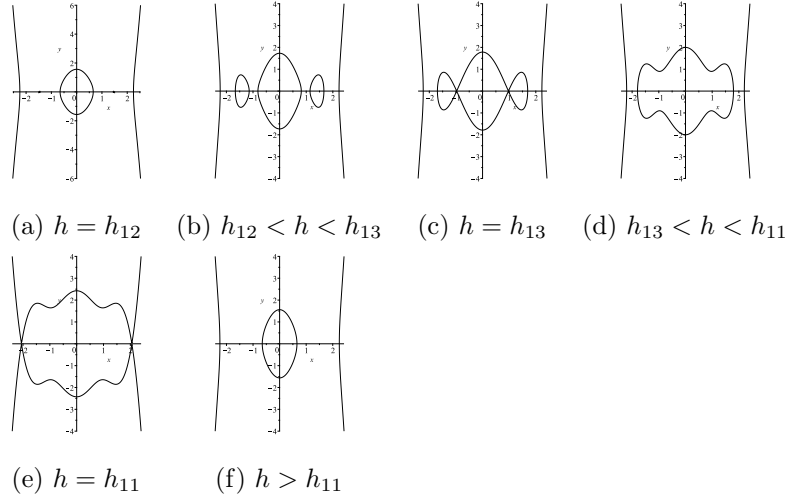
Figure 8 The changes of the level curves when $b_0 < 0, (b_2, b_4) \in \hat{I}_3, h_{11} > h_{13}$

When $h = h_{12}$, the level curves defined by $H_1(\phi, y) = h$ enclose two points $(\pm\phi_2, 0)$, a periodic orbit passing through ϕ−axis at the points $(\pm r_2, 0)$ and enclosing the origin, and two open curves passing through ϕ−axis at the points $(\pm r_1, 0)$ (Figure 8(a)). For the periodic orbit, we have $y^2 = \frac{1}{4}(r_1^2 - \phi^2)(\phi_2^2 - \phi^2)^2(r_2^2 - \phi^2)$. Substituting it into the first equation of system (2.6) and integrating along the periodic orbit, it follows that

$$\xi = \int_0^u \frac{du}{(\phi_2^2 - u)\sqrt{(r_1^2 - u)(r_2^2 - u)u}}.$$

Therefore, we have the parametric representation (4.8) of the periodic wave solution. The periodic solution has the following wave portrait Figure 9:
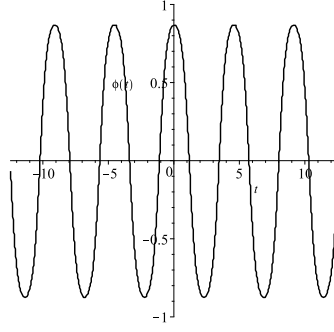
Figure 9 The periodic wave solution of system (2.6)

When $h = h_{13}$, the level curves defined by $H_1(\phi, y) = h$ are two heteroclinic orbits connecting to the equilibrium points $(\pm\phi_3, 0)$ and enclosing the origin, two homoclinic orbits to the points $(\pm\phi_3, 0)$ and passing through $\phi-$axis at the points $(\pm\phi_M, 0)$, and two open curves passing through $\phi-$axis at the points $(\pm r_1, 0)$ (Figure 8(c)). For the heteroclinic orbits, we have $y^2 = \frac{1}{4}(r_1^2 - \phi^2)(\phi_M^2 - \phi^2)(\phi_3^2 - \phi^2)^2$. Substituting it into the first equation of system (2.6) and integrating along the heteroclinic orbits, it follows that

$$\xi = \int_0^u \frac{du}{(\phi_3^2 - u)\sqrt{(r_1^2 - u)(\phi_M^2 - u)u}}.$$

Then, we have the parametric representations (4.9) of the kink and anti-kink solutions of system (2.6). Corresponding to the two homoclinic orbit loops, we have

$$\xi = \int_u^{\phi_M^2} \frac{du}{(u - \phi_3^2)\sqrt{(r_1^2 - u)(\phi_M^2 - u)u}}.$$

Therefore, the solitary wave solutions (4.10) are obtained.

(iv) When $b_0 < 0, (b_2, b_4) \in \hat{I}_3, h_{11} = h_{13}$, system (2.6) has phase portrait Figure 3(e). When $h = h_{11} = h_{13}$, the level curves defined by $H_1(\phi, y) = h$ are six heteroclinic orbits connecting to the points $(\pm\phi_1, 0)$ and $(\pm\phi_3, 0)$ and four stable and unstable manifolds of the equilibrium points $(\pm\phi_1, 0)$. Now, for the heteroclinic orbits which enclose the origin point, we have $y^2 = \frac{1}{4}(\phi^2 - \phi_1^2)^2(\phi^2 - \phi_3^2)^2$. Substituting it into the first equation of system (2.6) and integrating along the heteroclinic orbits, it follows that

$$\frac{1}{2}\xi = \int_0^\phi \frac{d\phi}{(\phi_1^2 - \phi^2)(\phi_3^2 - \phi^2)}.$$

Thus, we have the parametric representations (4.11) of heteroclinic solutions. For four heteroclinic orbits which enclose the equilibrium points $(\pm\phi_2, 0)$, we have

$$\frac{1}{2}\xi = \int_{\phi_2}^\phi \frac{d\phi}{(\phi_1^2 - \phi^2)(\phi^2 - \phi_3^2)}.$$

In this case, we obtain the parametric representations (4.12) of heteroclinic solutions.

(v) When $b_0 < 0, (b_2, b_4) \in \hat{I}_3, h_{11} < h_{13}$, system (2.6) has phase portrait Figure 3(f). When $h = h_{11}$, the level curves defined by $H_1(\phi, y) = h$ contain a periodic orbit enclosing the origin and passing through $\phi-$axis at the points $(\pm r_1, 0)$, two homoclinic orbits to the saddle points $(\pm \phi_1, 0)$ and passing through $\phi-$axis at the points $(\pm \phi_M, 0)$, and four stable and unstable manifolds of the equilibrium points $(\pm \phi_1, 0)$. Corresponding to the periodic orbit, we have $y^2 = \frac{1}{4}(\phi_1^2 - \phi^2)^2(\phi_M^2 - \phi^2)(r_1^2 - \phi^2)$. Substituting it into the first equation of system (2.6) and integrating along the periodic orbit, it follows that

$$\xi = \int_0^u \frac{du}{(\phi_1^2 - u)\sqrt{(\phi_M^2 - u)(r_1^2 - u)u}}.$$

Then, we have the parametric representation (4.13) of the periodic solution. Corresponding to the two homoclinic orbits, we have

$$\xi = \int_{\phi_M^2}^u \frac{du}{(\phi_1^2 - u)\sqrt{(u - \phi_M^2)(u - r_1^2)u}}.$$

Thus, we obtain the parametric representations (4.14) of the homoclinic orbits.   □

4.2. Exact parametric representations of solutions of system (2.7).

Theorem 4.3. *When $b_0 > 0$ (see Figure 4), system (2.7) has following traveling wave solutions:*

(i) When $b_0 > 0$, $(b_2, b_4) \in L_3$, system (2.7) has heteroclinic solutions

$$
\begin{aligned}
\phi(\chi) &= \pm \frac{r_1 k sn(\chi, k)}{dn(\chi, k)}, \quad \chi \in (-K, K), \\
\xi(\chi) &= \frac{2}{\phi_1^2(\phi_1^2 + r_1^2)^3}\left[\phi_1^2 \chi + r_1^2 \Pi(\arcsin(sn(\chi, k), 1, k))\right],
\end{aligned}
\tag{4.15}
$$

where $k^2 = \frac{\phi_1^2}{\phi_1^2 + r_1^2}$.

(ii) When $b_0 > 0$, $(b_2, b_4) \in I_3, h_{21} < 0$, system (2.7) has periodic wave solutions

$$
\begin{aligned}
\phi(\chi) &= \pm\left(\frac{r_3^2 k^2 sn^2(\chi, k) + r_2^2}{dn^2(\chi, k)}\right)^{\frac{1}{2}}, \\
\xi(\chi) &= \frac{2}{r_3^2(r_1^2 + r_3^2)^3}\left[-\chi + \frac{r_2^2 + r_3^2}{r_2^2}\Pi(\arcsin(sn(\chi, k)), \check{\alpha}_1^2, k)\right],
\end{aligned}
\tag{4.16}
$$

where $\check{\alpha}_1^2 = \frac{r_3^2(r_2^2 - r_1^2)}{r_2^2(r_1^2 + r_3^2)}, k^2 = \frac{r_1^2 - r_2^2}{r_1^2 + r_3^2}$.

In this case, system (2.7) also has heteroclinic solutions

$$
\begin{aligned}
\phi(\chi) &= \pm \frac{r_1 k sn(\chi, k)}{dn(\chi, k)}, \quad \chi \in \left(-sn^{-1}\sqrt{\frac{\phi_2^2(\phi_M^2 + r_1^2)}{\phi_M^2(r_1^2 + \phi_2^2)}}, sn^{-1}\sqrt{\frac{\phi_2^2(\phi_M^2 + r_1^2)}{\phi_M^2(r_1^2 + \phi_2^2)}}\right), \\
\xi(\chi) &= \frac{2}{(r_1^2 + \phi_2^2)(\phi_M^2 + r_1^2)}\left[\chi + \frac{r_1^2}{\phi_2^2}\Pi(\arcsin(sn(\chi, k)), \check{\alpha}_2^2, k)\right],
\end{aligned}
\tag{4.17}
$$

where $\check{\alpha}_2^2 = \frac{\phi_M^2(r_1^2 + \phi_2^2)}{\phi_2^2(r_1^2 + \phi_M^2)}, k^2 = \frac{\phi_M^2}{\phi_M^2 + r_1^2}$, and homoclinic solutions

$$
\begin{aligned}
\phi(\chi) &= \pm \phi_M cn(\chi, k), \quad \chi \in \left(-cn^{-1}(\frac{\phi_2}{\phi_M}), cn^{-1}(\frac{\phi_2}{\phi_M})\right), \\
\xi(\chi) &= \frac{2}{(\phi_M^2 - \phi_2^2)(\phi_M^2 + r_1^2)}\Pi(\arcsin(sn(\chi, k), \check{\alpha}_3^2, k)),
\end{aligned}
\tag{4.18}
$$

where $\check{\alpha}_3^2 = \frac{\phi_M^2}{\phi_M^2 - \phi_2^2}, k^2 = \frac{\phi_M^2}{\phi_M^2 + r_1^2}$.

(iii) When $b_0 > 0$, $(b_2, b_4) \in I_3$, $h_{21} > 0$, system (2.7) has periodic orbit solution

$$
\begin{aligned}
\phi(\chi) &= \pm\left(\frac{kr_2\,sn(\chi,k)}{dn(\chi,k)}\right), \\
\xi(\chi) &= \frac{2}{(r_2^2+\phi_1^2)(r_1^2+r_2^2)}\left[\chi + \frac{r_2^2}{\phi_1^2}\Pi(\arcsin(sn(\chi,k)), \check{\alpha}_4^2, k)\right],
\end{aligned}
\tag{4.19}
$$

where $\check{\alpha}_4^2 = \frac{r_1^2(r_2^2+\phi_1^2)}{\phi_1^2(r_1^2+r_2^2)}, k^2 = \frac{r_1^2}{r_1^2+r_2^2}$.

Proof. (i) When $b_0 > 0$, $(b_2, b_4) \in L_3$, system (2.7) has phase portrait Figure 4(b). When $h = h_{21} = h_{22}$, the level curves defined by $H_2(\phi, y) = h$ are two heteroclinic orbits connecting to the cusps $(\pm\phi_1, 0)$ and enclosing the origin. Now, for the heteroclinic orbits, we have $y^2 = \frac{1}{4}(\phi_1^2 - \phi^2)^3(\phi^2 + r_1^2)$. Substituting it into the first equation of system (2.7) and integrating along the heteroclinic orbits, it follows that

$$
\frac{1}{2}\xi = \int_0^\phi \frac{d\phi}{(\phi_1^2 - \phi^2)\sqrt{(\phi_1^2 - \phi^2)(\phi^2 + r_1^2)}}.
$$

Therefore, we have the parametric representations (4.15) of kink and anti-kink solutions.

(ii) When $b_0 > 0$, $(b_2, b_4) \in I_3$, $h_{21} < 0$, system (2.7) has portrait Figure 4(c). The changes of the level curves defined by $H_2(\phi, y) = h$ are shown as follows:

(a) $h_{21} < h < 0$ (b) $h = 0$ (c) $0 < h < h_{22}$ (d) $h = h_{22}$ (e) $h > h_{22}$
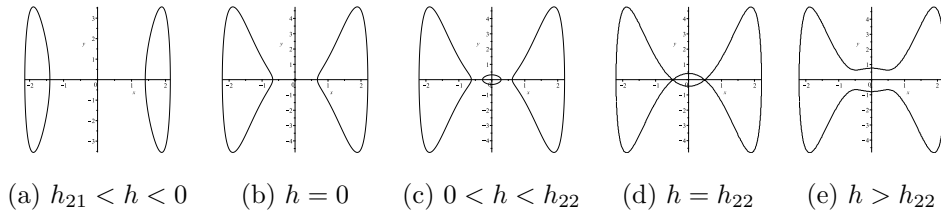
Figure 10 The changes of the level curves when $b_0 > 0$, $(b_2, b_4) \in I_3$, $h_{21} < 0$

When $h = 0$, the level curves defined by $H_2(\phi, y) = h$ contain the origin and two periodic orbits which enclose the center points $(\pm\phi_1, 0)$ and pass through $\phi-$axis at the points $(\pm r_1, 0)$ and $(\pm r_2, 0)$ (Figure 10(b)). Corresponding to the above periodic orbits, we have $y^2 = \frac{1}{4}(r_1^2 - \phi^2)(\phi^2 - r_1^2)\phi^2(\phi^2 + r_3^2)$, Substituting it into the first equation of system (2.7) and integrating along the periodic orbits, it follows that

$$
\xi = \int_{r_2^2}^u \frac{du}{u\sqrt{(r_1^2 - u)(u - r_2^2)(u + r_3^2)}}.
$$

Therefore, the two periodic orbits have the parametric representations (4.16). The two periodic wave solutions have the following wave portrait Figure 11:

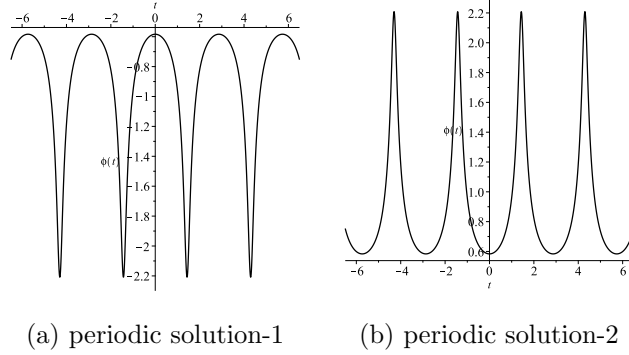(a) periodic solution-1   (b) periodic solution-2

Figure 11 The periodic wave solutions

When $h = h_{22}$, the level curves defined by $H_2(\phi, y) = h$ are two heteroclinic orbits connecting to the equilibrium points $(\pm\phi_2, 0)$ and two homoclinic orbits to the saddle points $(\pm\phi_2, 0)$ which pass through ϕ−axis at the points $(\pm\phi_M, 0)$ and enclose the the center points $(\pm\phi_1, 0)$. Now, for the heteroclinic orbits, we have $y^2 = \frac{1}{4}(\phi_M^2 - \phi^2)(\phi_2^2 - \phi^2)(\phi^2 + r_1^2)$. Substituting it into the first equation of system (2.7) and integrating along the heteroclinic orbits, it follows that

$$\xi = \int_0^u \frac{du}{(\phi_2^2 - u)\sqrt{(\phi_M^2 - u)u(u + r_1^2)}}.$$

Thus, we have the parametric representations (4.17) of kink and anti-kink solutions. For the homoclinic orbit loops, we have

$$\xi = \int_u^{\phi_M^2} \frac{du}{(u - \phi_2^2)\sqrt{(\phi_M^2 - u)u(u + r_1^2)}}.$$

Therefore, we obtain the parametric representations (4.18) of solitary wave solutions.

(iii) When $b_0 > 0$, $(b_2, b_4) \in I_3$, $h_{21} > 0$, system (2.7) has portrait Figure 4(e). When $h = h_{21}$, the level curves defined by $H_2(\phi, y) = h$ contain two equilibrium points $(\pm\phi_1, 0)$ and a periodic orbit enclosing the origin and passing through ϕ−axis at the points $(\pm r_1, 0)$. Corresponding to the above periodic orbit, we have $y^2 = \frac{1}{4}(\phi^2 - \phi_1^2)^2(r_1^2 - \phi^2)(\phi^2 + r_2^2)$, Substituting it into the first equation of system (2.7) and integrating along the periodic orbit, it follows that

$$\xi = \int_0^u \frac{du}{(\phi_1^2 - u)\sqrt{(r_1^2 - u)u(u + r_2^2)}}.$$

Thus, the periodic orbit has the parametric representation (4.19).   □

Theorem 4.4. *When $b_0 < 0$ (see Figure 5), system (2.7) has the following traveling wave solutions:*

(i) When $b_0 < 0$, $(b_2, b_4) \in \hat{I}_1$ or $(b_2, b_4) \in \hat{L}_1$ or $(b_2, b_4) \in \hat{I}_2$, system (2.7) has homoclinic solutions

$$\phi(\chi) = \pm\left(\frac{(A_2 + \phi_M^2)cn(\chi, k) + \alpha_M^2 - A_2}{1 + cn(\chi, k)}\right)^{\frac{1}{2}}, \quad \chi \in \left(-cn^{-1}(\frac{A_2 - \phi_M^2}{A_2 + \phi_M^2}), cn^{-1}(\frac{A_2 - \phi_M^2}{A_2 + \phi_M^2})\right),$$

$$\xi(\chi) = \frac{1}{(\phi_M^2 + A_2)A_2}\left\{\chi + \frac{\phi_M^2 - A_2}{2\phi_M^2}[\Pi(\arccos(cn(\chi, k)), \frac{\tilde{\alpha}_1^2}{\tilde{\alpha}_1^2 - 1}, k)) + \frac{\phi_M^2 + A_2}{2\phi_M^2}f_1]\right\}.$$

(4.20)

where $a_2^2 = -\frac{(\rho^2-\bar{\rho}^2)}{4}$, $b_2 = \frac{\rho^2+\bar{\rho}^2}{2}$, $A_2^2 = b_2^2 + a_2^2 = \rho^2\bar{\rho}^2$, $\tilde{\alpha}_1 = \frac{\phi_M^2+A_2}{\phi_M^2-A_2}$, $k^2 = \frac{A_2-b_2+\phi_M^2}{2A_2}$.

(ii) When $b_0 < 0$, $(b_2, b_4) \in \hat{L}_2$, system (2.7) has homoclinic solutions

$$\phi(\chi) = \pm\phi_M \, dn(\chi, k), \chi \in \left(-dn^{-1}(\frac{\phi_2}{\phi_M}), dn^{-1}(\frac{\phi_2}{\phi_M})\right),$$
$$\xi(\chi) = \frac{2}{\phi_M(\phi_M^2-\phi_2^2)}\Pi(\arcsin(sn(\chi,k)), 1, k). \tag{4.21}$$

where $k^2 = \frac{\phi_M^2-\phi_2^2}{\phi_M^2}$.

(iii) When $b_0 < 0$, $(b_2, b_4) \in \hat{I}_3, h_{21} < h_{23}$, system (2.7) has periodic wave solutions

$$\phi(\chi) = \pm\frac{r_2}{dn(\chi,k)},$$
$$\xi(\chi) = \frac{2}{r_1\phi_1^2}\left[-\chi + \frac{r_2^2}{r_2^2-\phi_3^2}\Pi(\arcsin(sn(\chi,k)), \tilde{\alpha}_2^2, k)\right]. \tag{4.22}$$

where $\tilde{\alpha}_2^2 = \frac{\phi_3^2(r_2^2-r_1^2)}{r_1^2(r_2^2-\phi_3^2)}, k^2 = \frac{r_1^2-r_2^2}{r_1^2}$, and homoclinic solutions

$$\phi(\chi) = \pm\phi_M \, dn(\chi, k), \chi \in \left(-dn^{-1}(\frac{\phi_2}{\phi_M}), dn^{-1}(\frac{\phi_2}{\phi_M})\right)$$
$$\xi(\chi) = \frac{2}{\phi_M(\phi_M^2-\phi_2^2)}\Pi(\arcsin(sn(\chi,k)), \tilde{\alpha}_3^2, k). \tag{4.23}$$

where $\tilde{\alpha}_3^2 = \frac{\phi_M^2-\phi_m^2}{\phi_M^2-\phi_2^2}, k^2 = \frac{\phi_M^2-\phi_m^2}{\phi_M^2}$.

$$\phi(\chi) = \pm\frac{\phi_m}{dn(\chi,k)}, \chi \in \left(-dn^{-1}(\frac{\phi_m}{\phi_M}), dn^{-1}(\frac{\phi_m}{\phi_M})\right)$$
$$\xi(\chi) = \frac{2}{\phi_M\phi_2^2}\left[\chi - \frac{\phi_m^2}{\phi_m^2-\phi_2^2}\Pi(\arcsin(sn(\chi,k)), \tilde{\alpha}_4^2, k)\right]. \tag{4.24}$$

where $\tilde{\alpha}_4^2 = \frac{\phi_2^2(\phi_M^2-\phi_m^2)}{\phi_M^2(\phi_2^2-\phi_m^2)}, k^2 = \frac{\phi_M^2-\phi_m^2}{\phi_M^2}$.

(iv) When $b_0 < 0$, $(b_2, b_4) \in \hat{L}_3$, system (2.7) has heteroclinic solutions

$$\phi(\chi) = \pm\frac{r_1 k sn(\chi,k)}{dn(\chi,k)}, \chi \in (-K, K)$$
$$\xi(\chi) = \frac{2}{\phi_1^2(\phi_1^2+r_1^2)}\left[\phi_1^2\chi + r_1^2\Pi(\arcsin(sn(\chi,k)), 1, k)\right], \tag{4.25}$$

where $k^2 = \frac{\phi_1^2}{\phi_1^2+r_1^2}$.

Proof. (i) When $b_0 < 0$, $(b_2, b_4) \in \hat{I}_1$ or $(b_2, b_4) \in \hat{L}_1$ or $(b_2, b_4) \in \hat{I}_2$, system (2.7) has phase portrait Figure 5(a). When $h = 0$, the level curves defined by $H_2(\phi, y) = h$ are two homoclinic orbits to the origin which pass through $\phi-$axis at the points $(\pm\phi_M, 0)$ and enclose the the center points $(\pm\phi_1, 0)$. Now, for the homoclinic orbits, we have $y^2 = \frac{1}{4}\phi^2(\phi_M^2 - \phi^2)(\phi^2 - \rho^2)(\phi^2 - \bar{\rho}^2)$, where ρ and $\bar{\rho}$ are two conjugated complex zeros of (4.1). Substituting it into the first equation of system (2.7) and integrating along the homoclinic orbits, it follows that

$$\xi = \int_u^{\phi_M^2} \frac{du}{u\sqrt{(\phi_M^2 - u)(\phi^2 - \rho^2)(\phi^2 - \bar{\rho}^2)}}.$$

Then, we obtain the parametric representations (4.20) of the homoclinic solutions.

(ii) When $b_0 < 0$, $(b_2, b_4) \in \hat{L}_2$, system (2.7) has phase portrait Figure 5(c). When $h = h_{22} = h_{23}$, the level curves defined by $H_2(\phi, y) = h$ are two homoclinic orbits to the cusps $(\pm\phi_2, 0)$ which pass through $\phi-$axis at the points $(\pm\phi_M, 0)$ and enclose the the center points $(\pm\phi_1, 0)$. Corresponding to the homoclinic orbits, we have $y^2 = \frac{1}{4}(\phi^2 - \phi_2^2)^3(\phi_M^2 - \phi^2)$, Substituting it into the first equation of system (2.7) and integrating along the homoclinic orbits, it follows that

$$\frac{1}{2}\xi = \int_\phi^{\phi_M} \frac{d\phi}{(\phi^2 - \phi_2^2)\sqrt{(\phi^2 - \phi_2^2)(\phi_M^2 - \phi^2)}}.$$

Therefore, the above homoclinic orbits have the parametric representations (4.21)

(iii) When $b_0 < 0$, $(b_2, b_4) \in \hat{I}_3$, $h_{21} < h_{23}$, system (2.7) has phase portrait Figure 5(d). The changes of the level curves $H_2(\phi, y) = h$ are shown as follows in Figure 12:

(a) $h_{21} < h < h_{23}$ (b) $h = h_{23}$ (c) $h_{23} < h < h_{22}$ (d) $h = h_{22}$

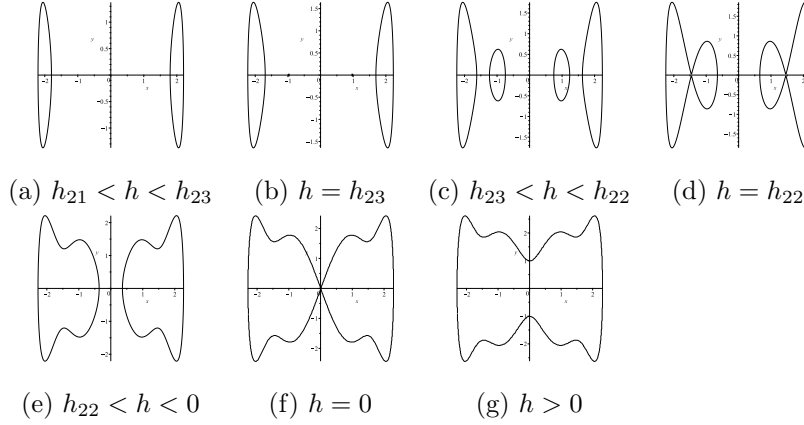(e) $h_{22} < h < 0$ (f) $h = 0$ (g) $h > 0$

Figure 12 The changes of the level curves when $b_0 < 0$, $(b_2, b_4) \in \hat{I}_3$, $h_{21} < h_{23}$

When $h = h_{23}$, the level curves defined by $H_2(\phi, y) = h$ contain two equilibrium points $(\pm\phi_3, 0)$, two periodic orbits which enclose the center points $(\pm\phi_1, 0)$ and pass through $\phi-$axis at the points $(\pm r_1, 0)$ and $(\pm r_2, 0)$ (Figure 12(b)). For the periodic orbits, we have $y^2 = \frac{1}{4}(\phi^2 - \phi_3^2)^2(r_1^2 - \phi^2)(\phi^2 - r_2^2)$, Substituting it into the first equation of system (2.7) and integrating along the periodic orbits, it follows that

$$\xi = \int_{r_2^2}^{u} \frac{du}{(u - \phi_1^2)\sqrt{(r_1^2 - \phi^2)(\phi^2 - r_2^2)}}.$$

Thus, we have the parametric representations (4.22) of the two periodic orbits.

When $h = h_{22}$, the level curves defined by $H_2(\phi, y) = h$ are four homoclinic orbits to the saddle points $(\pm\phi_2, 0)$ which pass through $\phi-$axis at the points $(\pm\phi_M, 0)$ and $(\pm\phi_m, 0)$ (Figure 12(d)). Corresponding to the homoclinic orbits enclosing the the center points $(\pm\phi_1, 0)$, we have $y^2 = \frac{1}{4}(\phi_M^2 - \phi^2)(\phi^2 - \phi_2^2)^2(\phi^2 - \phi_m^2)$, Substituting it into the first equation of system (2.7) and integrating along the homoclinic orbits, it follows that

$$\xi = \int_u^{\phi_M^2} \frac{du}{(u - \phi_2^2)\sqrt{(\phi_M^2 - u)(u - \phi_m^2)u}}.$$

Thus, the parametric representations (4.23) of the two homoclinic are obtained. Corresponding to the homoclinic orbits enclosing the the center points $(\pm\phi_3, 0)$, we have

$$\xi = \int_{\phi_m^2}^{u} \frac{du}{(\phi_2^2 - u)\sqrt{(\phi_M^2 - u)(u - \phi_m^2)u}}.$$

Then, we obtain the parametric representations (4.24) of the two homoclinic solutions.

(iv) When $b_0 < 0$, $(b_2, b_4) \in \hat{L}_3$, system (2.7) has phase portrait Figure 5(g). When $h = h_{21} = h_{22}$, the level curves defined by $H_2(\phi, y) = h$ are two heteroclinic orbits to the cusps $(\pm\phi_1, 0)$. For the above heteroclinic orbits, we have $y^2 = \frac{1}{4}(\phi_1^2 - \phi^2)^3(\phi^2 + r_1^2)$. Substituting it into the first equation of system (2.7) and integrating along the heteroclinic orbits, it follows that

$$\frac{1}{2}\xi = \int_{0}^{\phi} \frac{d\phi}{(\phi_1^2 - \phi^2)\sqrt{(\phi_1^2 - \phi^2)(\phi^2 + r_1^2)}}.$$

Therefore, we have the kink and anti-kink solutions (4.25). $\square$

5. Conclusion

In this paper, by employing the dynamic systems approach, we study all possible bifurcations of system (2.6) and system (2.7), and prove that the two systems have 24 different exact explicit solutions. These solutions give rise to 24 different exact traveling wave solutions for equation (1.1). Our results are very helpful for the physical applications of the equation, which governs the propagation of Raman solitons through optical metamaterials. In our future work, we will consider the solitons propagation equations with other perturbation terms, study their bifurcations and traveling wave solutions, and obtain more abundant dynamic behaviors of these solutions for governing equations.

Acknowledgements

References

[1] A. Biswas, R. Kaisar, K. R. Khan, M. F. Mahmood and M. Belic, *Bright and dark solitons in optical metamaterials*, Optik, 2014, 125(13), 3299–3302.

[2] A. Biswas, A. Mirzazadeh, M. Savescu, D. Milovic, K. R. Khan, M. F. Mahmood and M. Belich, *Singular solitons in optical metamaterials by ansatz method and simplest equation approach*, Journal of Modern Optics, 2014, 61(19), 1550–1555.

[3] A. Biswas, M. Mirzazadeh, M. Eslami, D. Milovic and M. Belic, *Solitons in Optical Metamaterials by Functional Variable Method and First Integral Approach*, Frequenz, 2014, 68(11-12), 525–530.

[4] P. F. Byrd and M. D. Fridman, *Handbook of Elliptic Integrals for Engineers and Sciensists*, Springer, Berlin, 1971.

[5] A. Hasegawa, *Optical solitons in fibers*, Springer, Berlin, 1989.

[6] E. V. Krishnan, M. A. Gabshi, Q. Zhou, K. R. Khan, M. F. Mahmood, Y. Xu, A. Biswas and M. Belic, *Solitons in Optical Metamaterials by Mapping Method*, Journal of Optoelectronics and Advanced Materials, 2015, 17(6), 511–516.

[7] J. Li, *Singular Nonlinear Traveling Wave Equations: Bifurcations and Exact Solutions*, Science Press, Beijing, 2013.

[8] J. Li, *Geometric Properties and Exact Travelling WaveSolutions for the Generalized Burger-FisherEquation and the Sharma-Tasso-Olver Equation*, Journal of Nonlinear Modeling and Analysis, 2019, 1(1), 1–10.

[9] J. Li and G. Chen, *Bifurcations of travelling wave solutions for four classes of nonlinear wave equations*, International Journal of Bifurcation and Chaos, 2005, 15(12), 3973–3998.

[10] J. Li and G. Chen, *On a class of singular nonlinear traveling wave equations*, International Journal of Bifurcation and Chaos, 2007, 17(11), 4049–4065.

[11] J. Li, Y. Zhang and X. Zhao, *On a class of singular nonlinear traveling wave equations(II): an example of GCKdV equations*, International Journal of Bifurcation and Chaos, 2009, 19(6), 1955–2007.

[12] J. Li, W. Zhou and G. Chen, *Understanding peakons, periodic peakons and compactons via a shallow water wave equation*, International Journal of Bifurcation and Chaos, 2016, 26(12), 1650207.

[13] C. V. Raman, *A New Radiation*, Indian Journal of Physics, 1928, 2, 387–398.

[14] V. M. Shalaev, *Optical Negative-Index Metamaterials*, Nature, Photonics, 2007, 1, 41–48.

[15] D. R. Smith, W. J. Padilla, D. C. Vier, S. C. Nemat-Nasser and S. Schultz, *Composite medium with simultaneously negative permeability and permittivity*, Physical Review Letters, 2000, 84(18), 4184–4187.

[16] A. Sonmezoglu, M. Yao, M. Ekici, M. Mirzazadeh and Q. Zhou, *Explicit solitons in the parabolic law nonlinear negative-index materials*, Nonlinear Dynamics, 2017, 88, 595–607.

[17] M. Veljkovic, Y. Xu, D. Milovic, M. F. Mahmood, A. Biswas and M. R. Belic, *Super-Gaussian Solitons in Optical Metamaterials using Collective Variables* Journal of Computational and Theoretical Nanoscience, 2015, 12(12), 5119–5124.

[18] Y. Xiang, X. Dai, S. Wen, J. Guo and D. Fan, *Controllable Raman soliton self-frequencyshift in nonlinear metamaterials*, Physical Review Letters, 2011, 84(3), 033815.

[19] Y. Xu, P. Pablo Suarez, D. Milovic, K. R. Khan, M. F. Mahmood, A. Biswas and M. Belic, *Raman solitons in nanoscale optical waveguides, with metamaterials, having polynomial law nonlinearity*, Journal of Modern Optics, 2016, 63(53), 532–537.

[20] Y. Xu, Q. Zhou, A. Bhrawy, K. R. Khan, M. F. Mahmood, A. Biswas and M. R. Belic, *Bright Solitons in Optical Metamaterials by Traveling Wave Hypothesis*

Optoelectronics and Advanced Materials-Rapid Communications, 2015, 9(3), 384.

[21] Y. Zhou, *Exact Solutions and Dynamics of the Raman Soliton Model in Nanoscale Optical Waveguides, with Metamaterials, Having Parabolic Law Non-Linearity*, Journal of Applied Analysis and Computation, 2018, 9(1), 159–186.

[22] Y. Zhou and J. Li, *Exact Solutions and Dynamics of the Raman Soliton Model in Nanoscale Optical Waveguides, with Metamaterials, Having Polynomial Law Non-Linearity*, International Journal of Bifurcation and Chaos, 2017, 27(12), 1750188.